Follow us @BoneJointRes

Freely available online OPEN ACCESS

BJR

BONE BIOLOGY

Hsa_circ_0066523 promotes the proliferation and osteogenic differentiation of bone mesenchymal stem cells by repressing PTEN

W. Xin,
S. Yuan,
B. Wang,
Q. Qian,
Y. Chen

From Changzheng Hospital, Shanghai, China

Aims

Circular RNAs (circRNAs) are a novel type of non-coding RNA that plays major roles in the development of diverse diseases including osteonecrosis of the femoral head (ONFH). Here, we explored the impact of hsa_circ_0066523 derived from forkhead box P1 (FOXP1) (also called circFOXP1) on bone mesenchymal stem cells (BMSCs), which is important for ONFH development.

Methods

RNA or protein expression in BMSCs was analyzed by quantitative real-time polymerase chain reaction (qRT-PCR) or western blot, respectively. Cell Counting Kit 8 (CCK8) and 5-ethynyl-2'-deoxyuridine (EdU) were used to analyze cell proliferation. Alkaline phosphatase (ALP) activity, ALP staining, and Alizarin Red S staining were employed to evaluate the osteoblastic differentiation. Chromatin immunoprecipitation (ChIP), luciferase reporter, RNA pull down, and RNA immunoprecipitation (RIP) assays were combined for exploring molecular associations.

Results

Circ_0066523 was upregulated in osteogenic induction process of BMSCs. Silencing circ_0066523 restrained the proliferation and osteogenic differentiation of BMSCs. Mechanistically, circ_0066523 activated phosphatidylinositol-4,5-bisphosphate 3-kinase / AKT serine/threonine kinase 1 (PI3K/AKT) pathway via recruiting lysine demethylase 5B (KDM5B) to epigenetically repress the transcription of phosphatase and tensin homolog (PTEN). Functionally, AKT signalling pathway agonist or PTEN knockdown counteracted the effects of silenced circ_0066523 on BMSC proliferation and differentiation.

Conclusion

Circ_0066523 promotes the proliferation and differentiation of BMSCs by epigenetically repressing PTEN and therefore activating AKT pathway. This finding might open new avenues for the identification of therapeutic targets for osteoblast differentiation related diseases such as ONFH.

Cite this article: *Bone Joint Res* **2021;10(8):526–535.**

Keywords: circ_0066523, Osteoblast differentiation, KDM5B

Article focus

- The relationship between circ_0066523 and bone mesenchymal stem cell (BMSC) osteogenic differentiation and proliferation was explored.
- The underlying mechanism of circ_0066523 in BMSCs was evaluated.

Key messages

- Circ_0066523 is overexpressed in the induction process of BMSC osteogenic differentiation.
- Circ_0066523 contributes to the proliferation and osteogenic differentiation of BMSCs via phosphatase and tensin homolog / phosphatidylinositol-4,5-bisphosphate

Correspondence should be sent to Bo Wang; email: bo3736033699@163.com

doi: 10.1302/2046-3758.108.BJR-2020-0127.R2

Bone Joint Res 2021;10(8):526–535.

3-kinase / AKT serine/threonine kinase 1 (PTEN/PI3K/AKT) pathway.
- Circ_0066523 recruits lysine demethylase 5B (KDM5B) to epigenetically repress the transcription of PTEN.

Strengths and limitations

- We discovered the high expression of circ_0066523 in the induction process of BMSC osteogenic differentiation for the first time.
- We verified that circ_0066523 promotes the proliferation and osteogenic differentiation of BMSCs by PTEN/PI3K/AKT pathway for the first time.
- We proved for the first time that circ_0066523 recruits KDM5B to epigenetically repress the transcription of PTEN.
- This study focused on the changes of cell function, which is fundamental in research of the disease, but lacked more in-depth exploration, especially clinical evidence; for example, the pathway that was discovered in vitro has yet to be tested in human disease. In the future, we will continue to study further in this direction.

Introduction

Osteonecrosis of the femoral head (ONFH) is a bone-destructive disease that mainly occurs in the weight-bearing area of the femoral head. It usually affects people aged from 30 to 50 years. It has been reported that the altered osteogenic differentiation of bone mesenchymal stem cells (BMSCs) is an essential factor in the development of non-traumatic ONFH.[1] Furthermore, previous research unveiled that many factors can affect the osteogenic differentiation of BMSCs, such as parathyroid hormone 1-34,[2] Staphylococcal enterotoxin C2,[3] and so on. However, the biomarkers or therapeutic targets for ONFH are still lacking.

Recently, non-coding RNAs (ncRNAs), a type of RNA transcript without abilities to encode proteins, have been found to be implicated in various human diseases including osteonecrosis.[4] In addition, reports have also indicated the involvement of ncRNAs in regulating the proliferation and osteoblast differentiation of mesenchymal stem cells (MSCs).[5] Characterized by a covalently closed continuous conformation, circular RNAs (circRNAs) are a newly discovered subtype of ncRNA family.[6,7] They have been increasingly reported to induce regulatory effects on a wide array of cellular activities, such as cell proliferation,[8] invasion,[9] and differentiation.[10] MicroRNA (miRNA) sponge, transcription mediation, and interaction with RNA-binding proteins (RBPs) are the primary regulatory mechanisms of circRNAs. The critical role of circRNAs in bone diseases has been unveiled already. For example, circular RNA runt-related transcription factor 2 (circ_RUNX2) was experimentally proved to regulate osteoporosis via sponging miR-203 to elevate RUNX2 expression in human BMSCs.[11] However, the potential functions of majority circRNAs are still poorly investigated. Previously, a circRNA from FOXP1 (hsa_circ_0001320) was suggested to control the identity and differentiation of MSCs.[12] Further, it was validated to facilitate osteogenic differentiation in osteoporosis through targeting miR-33a-5p/FOXP1 signalling.[13] Hsa_circ_0066523, a novel circRNA, also originated from FOXP1 (hence also known as circFOXP1), has never been studied in any diseases. In this work, the expression of circ_0066523 was explored in the osteogenic induction process of BMSCs by preliminary experiments. Also, the precise influences of circ_0066523 on BMSCs and its underlying mechanism need to be investigated further.

Phosphatidylinositol-4,5-bisphosphate 3-kinase / AKT serine/threonine kinase 1 (PI3K/AKT) signalling is identified as a crucial intracellular pathway in multiple diseases.[14] Of note, this pathway has already been uncovered to play a critical role in various biological activities of osteoblast, including osteoblast differentiation, maturation, and bone growth.[15-17] The importance of this pathway has also been indicated in bone diseases. For example, blocking PI3K/AKT signalling pathway could inhibit chondrocyte differentiation and longitudinal bone growth progression.[18] In osteoporosis, numerous studies also support the implication of PI3K/AKT signalling in the proliferation and osteogenic differentiation of BMSCs.[19,20] Nevertheless, whether circ_0066523 could affect PI3K/AKT pathway in BMSCs remains unknown.

In our study, we detected the expression of circ_0066523 in BMSCs after osteogenic induction. The role of circ_0066523 knockdown on BMSC proliferation and differentiation was analyzed via in vitro experiments. Mechanism exploration was performed to reveal the regulation between circ_0066523 and AKT pathway via circ_0066523 transcriptional repression on phosphatase and tensin homolog (PTEN) through recruiting lysine demethylase 5B (KDM5B). Our findings may provide new ideas for the treatment of BMSC-related bone diseases such as ONFH.

Methods

BMSC culture and osteogenic differentiation induction. Human bone mesenchymal stem cells (BMSCs; passage 2) were available from Cell Bank of the Chinese Academy of Sciences (China). BMSCs were grown in α-Minimum Essential Medium (MEM) (Invitrogen, Thermo Fisher Scientific, USA) containing 10% fetal bovine serum (FBS) and 1% penicillin/streptomycin at 37°C in 5% carbon dioxide (CO_2). For osteogenic differentiation induction, cells planted in a 12-well plate (5×10^5 cells/well) were treated for 14 days with 10 mM of β-glycerophosphate, 200 μM of ascorbic acid, and 100 nM of dexamethasone (all from MilliporeSigma, USA). The medium was changed every three days, and cells were tested at zero, seven, and 14 days.

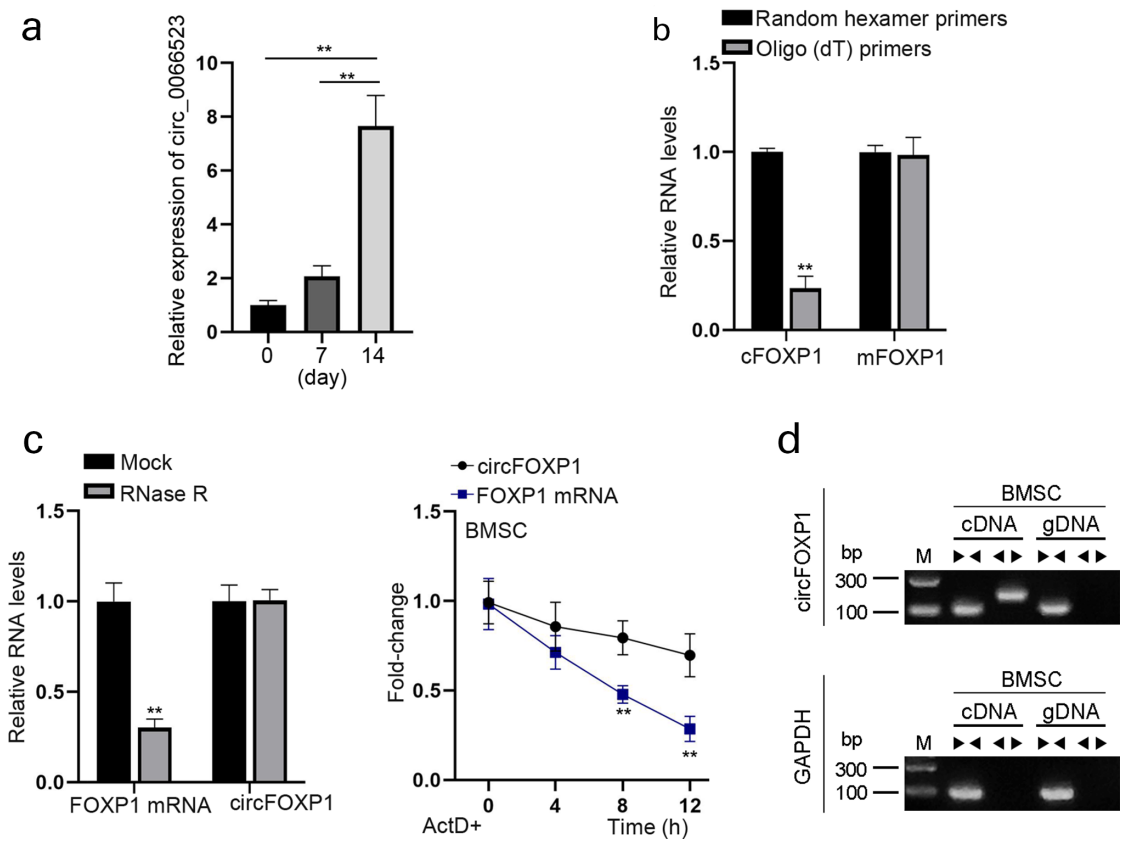

Fig. 1

Circ_0066523 is overexpressed in the osteoblast differentiation induction process of bone mesenchymal stem cells (BMSCs). a) The expression of circ_0066523 was evaluated by quantitative real-time polymerase chain reaction (qRT-PCR) in BMSCs treated with osteogenic differentiation medium for zero, seven, and 14 days. b) qRT-PCR assay measured the level of circFOXP1 (circ_0066523) and FOXP1 messenger RNA (mRNA) amplified by the primers of random hexamer or oligo (dT). c) qRT-PCR evaluated the levels of circ_0066523 and FOXP1 mRNA after RNase R or ActD treatment. d) Agarose gel electrophoresis analyzed the complementary DNA (cDNA) or genomic DNA (gDNA) products amplified by divergent or convergent primers. Lane 1 was added with the marker, Lane 2 was polymerase chain reaction (PCR) product amplified by convergent primers in cDNA, Lane 3 was PCR product amplified by divergent primers in cDNA, Lane 4 was PCR product amplified by convergent primers in gDNA, and Lane 5 was PCR product amplified by divergent primers in gDNA. **p < 0.01. cFOXP1, circFOXP1; GAPDH, glyceraldehyde-3-phosphate dehydrogenase; mFOXP1, FOXP1 messenger RNA.

Total RNA isolation and quantitative real-time polymerase chain reaction. Total RNAs were isolated from BMSCs using TRIzol (Invitrogen) following the manual's instructions. Complementary DNA (cDNA) was synthesized under the guidance of the supplier (TaKaRa, Japan). SYBR Premix Ex Taq (TaKaRa) was applied for quantification analysis, with U6 small nucleus RNA (snRNA) or glyceraldehyde-3-phosphate dehydrogenase (GAPDH) used as the normalized control. Relative expression level was calculated based on the $2^{-\Delta\Delta Ct}$ method.

Alizarin Red S staining. BMSCs were fixed with 70% ethanol and then stained with 2% Alizarin Red S (MilliporeSigma). After washing in phosphate-buffered saline (PBS), the images of stained cells were visualized under a light microscope (Leica Microsystems, Germany). For quantification of mineralization, cells were incubated for one hour with 1 ml of cetylpyridinium chloride buffer to extract Alizarin Red S. Afterwards, the level of Alizarin Red S in total protein was determined by monitoring the absorbance at 562 nm via a microplate reader (Thermo Fisher Scientific). Alizarin Red S accumulation was expressed as μmol/μg protein.

Alkaline phosphatase activity detection and staining. After removing culture medium, cells were rinsed in pre-warmed PBS. For alkaline phosphatase (ALP) activity detection, ALP activity colorimetric assay kit was available from BioVision (USA). The rinsed cells were lysed in 1% Triton X-100, scraped into distilled water, and finally assayed by microplate reader at 405 nm. For ALP staining, BMSCs were fixed by 4% paraformaldehyde (Sangon Biotech, China) and then stained in line with the direction (Gefan Biotechnology, China). Images were acquired using a light microscope (Leica Microsystems).

RNase R and actinomycin D treatment. A total of 2 mg of total RNA was prepared for incubation at 37°C with 3 U/mg of RNase R (Epicentre Technologies, USA) for 20 minutes or with 2 μg/ml of actinomycin D (ActD; MilliporeSigma) for 12 hours. After that, the levels of circ_0066523 or FOXP1 messenger RNA (mRNA) were examined by quantitative real-time polymerase chain reaction (qRT-PCR).

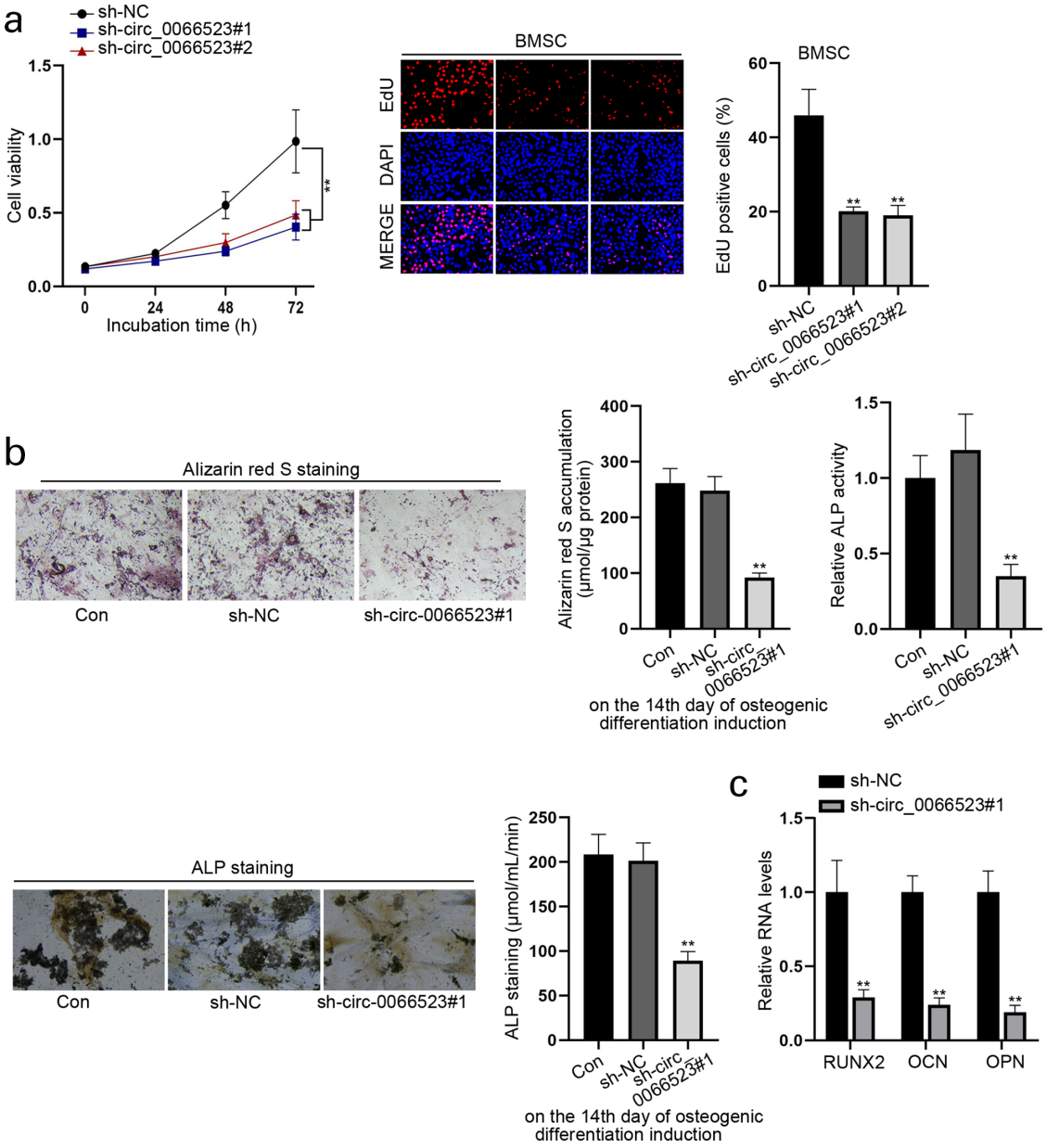

Fig. 2

Circ_0066523 knockdown hampers the proliferation and osteogenic differentiation of bone mesenchymal stem cells (BMSCs). a) Cell Counting Kit 8 (CCK8) and 5-ethynyl-2′-deoxyuridine (EdU) assays were performed for exploring BMSC proliferation after silencing of circ_0066523 (magnification 100×). b) After 14 days, osteogenic differentiation induction, Alizarin Red S staining, alkaline phosphatase (ALP) activity detection, and ALP staining were conducted in indicated BMSCs (magnification 200×). c) The levels of runt-related transcription factor 2 (RUNX2), osteopontin (OPN), and osteocalcin (OCN) were detected by quantitative real-time polymerase chain reaction (qRT-PCR) in BMSCs under different conditions. **p < 0.01. Con, control; DAPI, 4′,6-diamidino-2-phenylindole; sh-NC, negative control short hairpin RNA.

Plasmid transfection. The synthesized short hairpin RNAs (shRNAs) and negative control short hairpin RNAs (NC-shRNAs) for circ_0066523, KDM5B, or PTEN were acquired from GenePharma (China). For gene overexpression, KDM5B sequence was cloned into plasmid complementary DNA 3.1 (pcDNA3.1) vector (Invitrogen), while circ_0066523 sequence was subcloned into pcDNA3.1 (+) CircRNA Mini Vector (GenePharma). Lipofectamine 2000 (Invitrogen) was used for the transfection of the above plasmids into BMSCs for 48 hours.

Cell Counting Kit 8 assay. A total of 2 × 10^4 BMSCs were seeded into each well of a 96-well plate for overnight culture. Then, the plate was processed with Cell Counting Kit 8 (CCK8) solution (10 μl; Dojindo, Japan) for indicated times (zero, 24, 48, and 72 hours) at 37°C. After that, the plate was assayed by microplate reader to determine the absorbance at 450 nm.

***5-ethynyl-2′-deoxyuridine* incorporation assay.** The proliferation of 5 × 10^4 BMSCs was estimated by 5-ethynyl-2′-deoxyuridine (EdU) incorporation assay

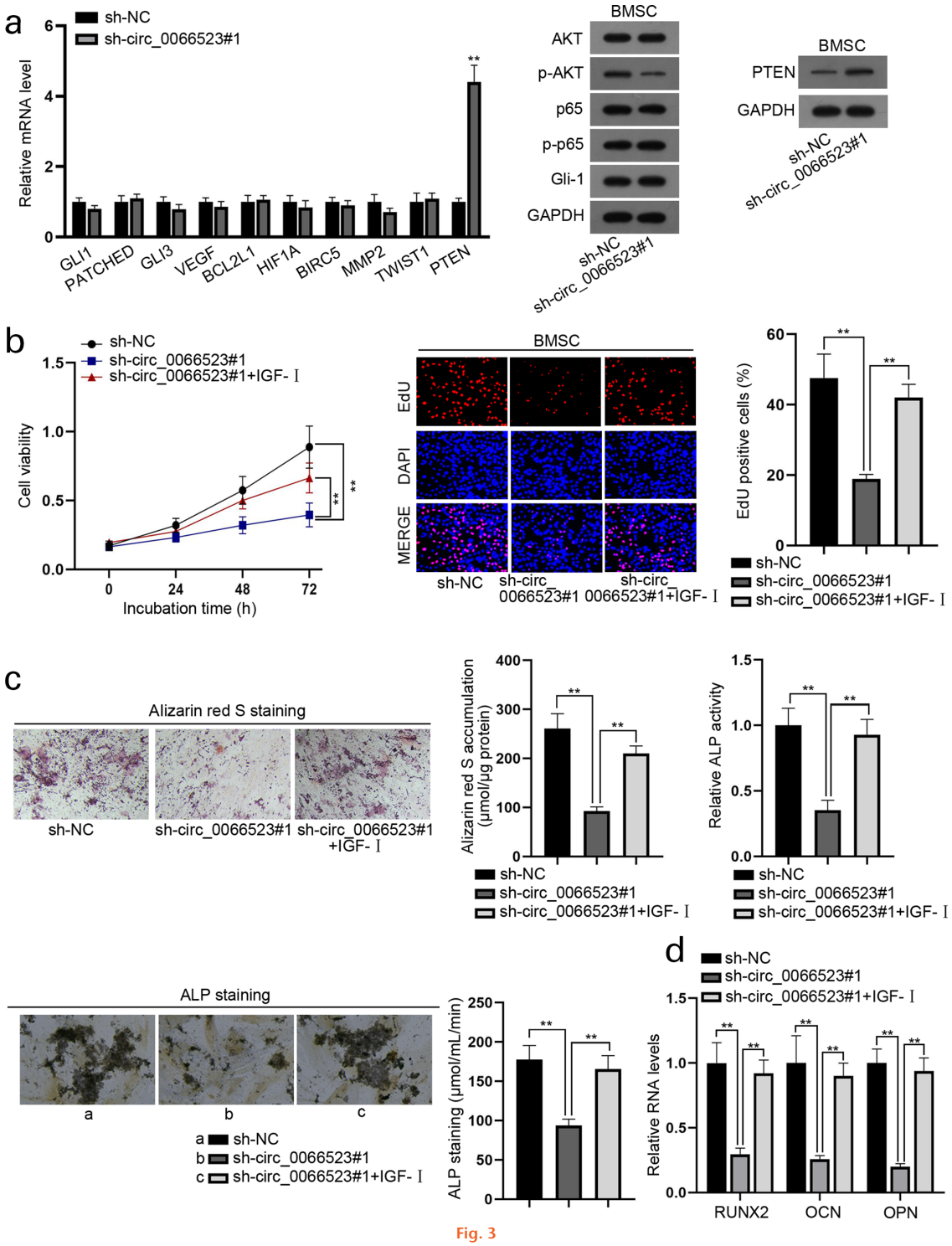

Fig. 3

The phosphatidylinositol-4,5-bisphosphate 3-kinase / AKT serine/threonine kinase 1 (PI3K/AKT) pathway mediates the regulation of circ_0066523 on bone mesenchymal stem cells (BMSCs). a) Quantitative real-time polymerase chain reaction (qRT-PCR) and western blot analyzed the expression level of genes related to Hedgehog, nuclear factor kappa-light-chain-enhancer of activated B cells (NF-κB), and PI3K/AKT pathways in BMSCs after the silencing of circ_0066523. b) Cell Counting Kit 8 (CCK8) and 5-ethynyl-2′-deoxyuridine (EdU) assays were performed to study the proliferation of transfected BMSCs (magnification 100×). c) Alizarin Red S staining, alkaline phosphatase (ALP) activity detection, and ALP staining examined changes in the differentiation of BMSCs under diverse conditions (magnification 200×). d) qRT-PCR analyzed the expression of runt-related transcription factor 2 (RUNX2), osteopontin (OPN), and osteocalcin (OCN) in indicated BMSCs. **p < 0.01. DAPI, 4′,6-diamidino-2-phenylindole; Gli-1, GLI family zinc finger 1; IGF-I, insulin-like growth factor 1; MMP, matrix metalloproteinase; mRNA, messenger RNA; PTEN, phosphatase and tensin homolog; sh-NC, negative control short hairpin RNA; VEGF, vascular endothelial growth factor.

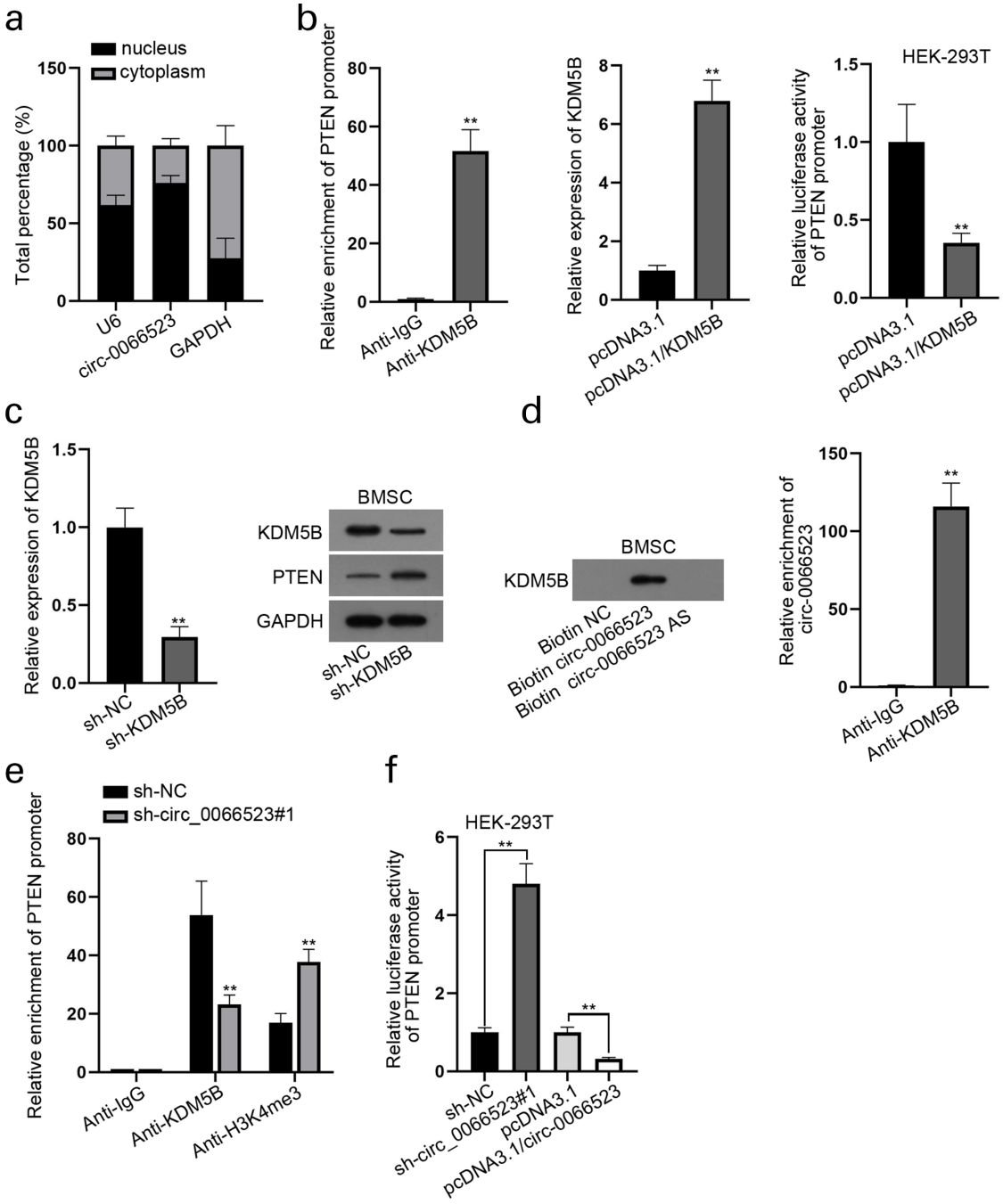

Fig. 4

Circ_0066523 recruits lysine demethylase 5B (KDM5B) to epigenetically repress the transcription of phosphatase and tensin homolog (PTEN). a) The distribution of circ_0066523 in bone mesenchymal stem cells (BMSCs) was detected by the subcellular fractionation assay. b) Chromatin immunoprecipitation (ChIP) assay testified the binding affinity between KDM5B and PTEN promoter; quantitative real-time polymerase chain reaction (qRT-PCR) tested the overexpression efficiency of plasmid complementary DNA 3.1 (pcDNA3.1)/KDM5B; luciferase reporter assay measured the luciferase activity of PTEN promoter in HEK-293T cells after KDM5B overexpression. c) qRT-PCR detected KDM5B messenger RNA (mRNA) expression, and western blot tested the protein levels of KDM5B and PTEN in BMSCs after sh-KDM5B transfection. d) RNA pull down and RIP assays determined the binding between KDM5B and circ_0066523 in BMSCs. e) ChIP assay explored the effects of circ_0066523 silencing on the occupancy of PTEN promoter by KDM5B and H3K4me3. f) Luciferase reporter assay was carried out in HEK-293T cells when circ_0066523 was silenced or overexpressed. **p < 0.01. GAPDH, glyceraldehyde-3-phosphate dehydrogenase; IgG, immunoglobulin G.

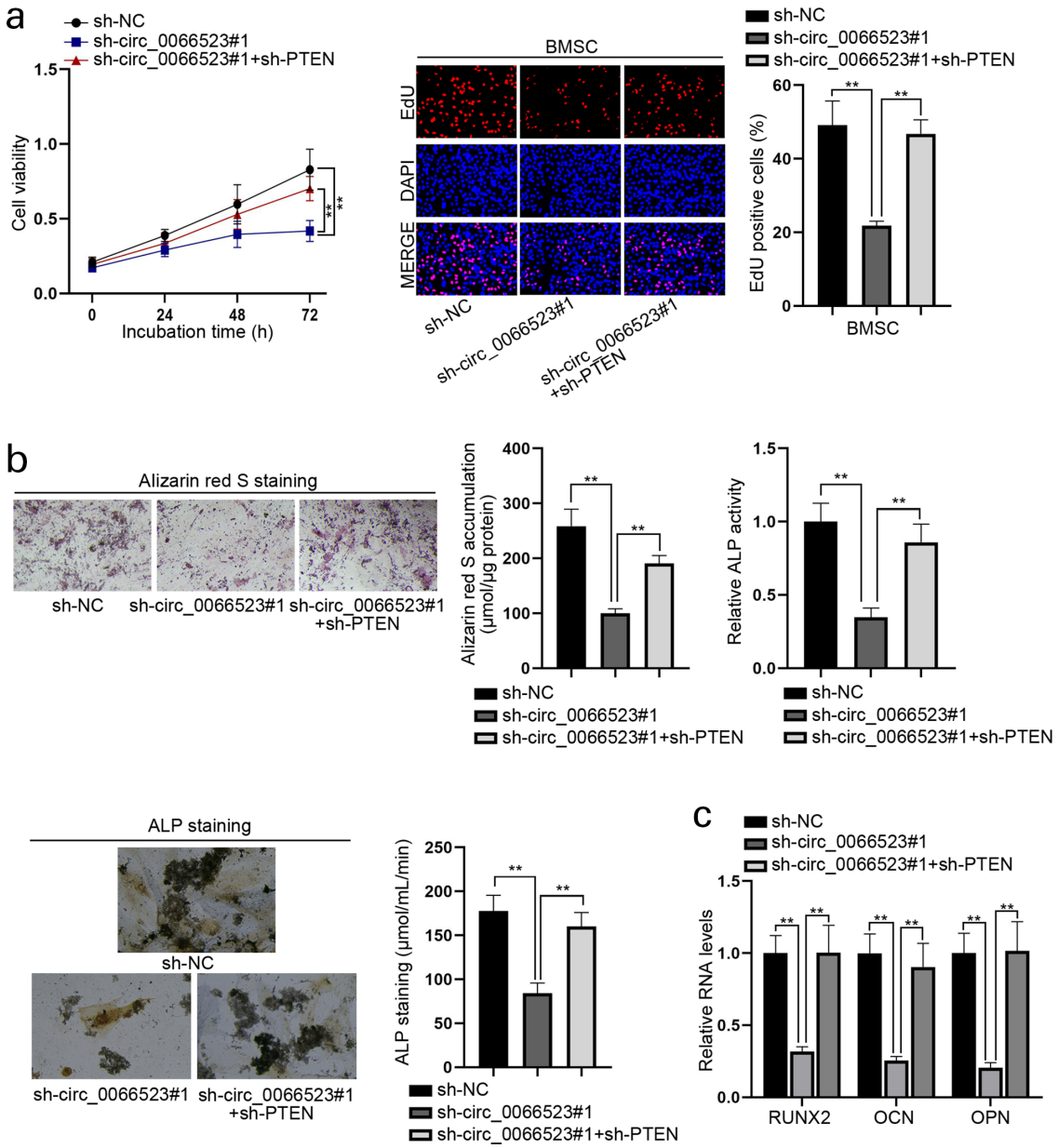

Fig. 5

Phosphatase and tensin homolog (PTEN) knockdown counteracts the effects of circ_0066523 interference on the behaviours of bone mesenchymal stem cells (BMSCs). a) The proliferation of indicated BMSCs was evaluated by Cell Counting Kit 8 (CCK8) and 5-ethynyl-2′-deoxyuridine (EdU) assays (magnification 100×). b) Alizarin Red S staining, alkaline phosphatase (ALP) activity assay, and ALP staining analyzed the osteoblastic phenotypes of transfected BMSCs (magnification 200×). c) The levels of runt-related transcription factor 2 (RUNX2), osteocalcin (OCN), and osteopontin (OPN) in indicated BMSCs were detected by quantitative real-time polymerase chain reaction (qRT-PCR). **p < 0.01. DAPI, 4′,6-diamidino-2-phenylindole; sh-NC, negative control short hairpin RNA.

reagent (RiboBio, China) in a 96-well plate. Simply put, cells were grown in the plate until 80% confluence and then treated with EdU reagent for four hours. After fixing and permeabilizing, cells were washed in PBS, dyed with 4′,6-diamidino-2-phenylindole (DAPI) solution, and then observed under a fluorescence microscope (Olympus, Japan).

Western blot. The extraction of total protein from BMSCs was achieved by using RIPA lysis buffer (Solarbio, China), and then protein concentration was determined via a bicinchoninic acid (BCA) kit (Pierce Biotechnology, Thermo Fisher Scientific). Subsequently, proteins were separated by 12% sodium dodecyl sulfate polyacrylamide gel electrophoresis (SDS-PAGE) and then shifted to poly(vinylidene fluoride) (PVDF) membranes, and then the membranes were blocked in 5% non-fat milk. Primary antibodies against GAPDH (loading control) and GLI family zinc finger 1 (Gli-1), p-p65, p65, p-AKT, AKT, PTEN, and KDM5B were diluted at 1:2,000 for incubation with membranes. After washing in TBS+Tween (TBST),

membranes were probed by the horseradish peroxidase (HRP)-labelled secondary antibodies (1:10,000 dilution), followed by the detection of protein signals via ECL detection system (Pierce, USA).

Subcellular fractionation. Subcellular fractionation assay was accomplished by PARIS Kit (Invitrogen). A total of 1 × 10^6 BMSCs were lysed in cell fractionation buffer before centrifugation to separate cytoplasmic and nuclear fractions. The isolated RNAs were assayed using qRT-PCR.

Chromatin immunoprecipitation. The formaldehyde cross-linked chromatin from BMSCs was sonicated into DNA fragments of 200-bp to 1,000-bp. The magnetic beads were bound with anti-KDM5B or anti-H3K4me3 antibody for immunoprecipitation. Normal mouse immunoglobulin G (IgG) antibody was used in the control group. The precipitated DNA was analyzed using qRT-PCR.

Luciferase reporter assay. After polymerase chain reaction (PCR) amplification, PTEN promoter was subcloned into the upstream of firefly gene in pGL3-basic luciferase vector (Promega, USA). For luciferase reporter assay, above recombinant pGL3 vector was cotransfected into HEK-293T cells with pcDNA3.1/KDM5B (or NC-pcDNA3.1), sh-circ_0066523 (or sh-NC), or pcDNA3.1/circ_0066523 (or NC-pcDNA3.1). After 48 hours, the luciferase activity was analyzed via Luciferase Reporter Assay System (Promega).

RNA pull down assay. Pierce Magnetic RNA-Protein Pull-Down Kit was acquired from Thermo Fisher Scientific for RNA pull down assay as instructed. The protein extracts were mixed with biotin-tagged circ_0066523 probes or negative control (NC) probe. Magnetic beads were added for collecting the pull-downs, followed by western blot detection of the interacting proteins.

RNA immunoprecipitation. Magna RIP RNA-Binding Protein Immunoprecipitation Kit was obtained from MilliporeSigma for RNA immunoprecipitation (RIP) assay. Magnetic beads were preincubated with anti-KDM5B or anti-IgG antibody for immunoprecipitation with cell lysates in RIP buffer. The purified RNA was finally subjected to qRT-PCR analysis.

Statistical analysis. Each experiment contained three independent bio-repeats to reduce experimental error. Results were given as means and standard deviations (SDs) and analyzed using GraphPad PRISM 6 (GraphPad, USA). Independent-samples *t*-test or one-way analysis of variance (ANOVA) was conducted for data analysis, with statistical significance defined as $p < 0.05$.

Results

Circ_0066523 is overexpressed in BMSCs under osteoblast differentiation induction. To understand the probable role of circ_0066523 in the osteoblast differentiation of BMSCs, we first studied the change of its expression during osteoblast differentiation induction. It was validated that three osteogenic marker genes (RUNX2, osteopontin (OPN), and osteocalcin (OCN)) were all gradually upregulated during the induction process of BMSC osteogenic differentiation (Supplementary Figure aa). Meanwhile, we discovered the increased mineralization, enhanced ALP activity, and increased ALP-positive blue-violet complexes during the induction process, certifying that the osteogenic differentiation of BMSCs was successfully induced (Supplementary Figures ab and ac). Interestingly, the results of qRT-PCR showed that circ_0066523 expression steadily increased with the induction duration (Figure 1a), indicating the potential positive role of circ_0066523 in BMSC osteogenic differentiation. Then, qRT-PCR assay showed that only FOXP1 mRNA, rather than circ_0066523 (circFOXP1), could be reverse transcribed by the primers for oligo (dT) (Figure 1b). Besides, we found that compared with FOXP1 mRNA, circ_0066523 exhibited a better resistance to RNase R and ActD treatment (Figure 1c). Furthermore, circ_0066523 was only amplified by divergent primers and detectable in cDNA but not genomic DNA (gDNA) (Figure 1d). These results prove the circular structure of circ_0066523. In summary, circ_0066523 is upregulated during the osteogenic differentiation process of BMSCs.

Circ_0066523 knockdown hampers the proliferation and osteogenic differentiation of BMSCs. To explore the biological influence of circ_0066523 on BMSCs, we silenced circ_0066523 in BMSCs by transfecting with sh-circ_0066523#1/2 for loss-of-function assays (Supplementary Figure ad). As a result, silencing circ_0066523 greatly hampered the proliferation of BMSCs (Figure 2a). We then probed into the effect of circ_0066523 deficiency on the osteoblastic phenotype of BMSCs, which underwent 14 days of induction. As expected, Alizarin Red S-stained mineralized nodules were lessened, and the ALP activity and ALP staining were attenuated after circ_0066523 depletion (Figure 2b). Moreover, we found that the levels of RUNX2, OPN, and OCN were all decreased after the depletion of circ_0066523 (Figure 2c). These results showed that knockdown of circ_0066523 inhibited the proliferation and differentiation of BMSCs.

PI3K/AKT pathway mediates the influence of circ_0066523 on BMSCs. Thereafter, we aimed to explore how circ_0066523 affects the function of BMSCs. We measured the expression changes in factors related to several important signalling pathways that have been reported to impact osteoblast activities, such as Hedgehog, nuclear factor kappa-light-chain-enhancer of activated B cells (NF-κB), and PI3K/AKT pathways. Intriguingly, we observed that loss of circ_0066523 elevated the levels of PTEN and decreased the level of p-AKT, indicating the activation of PI3K/AKT pathway, while the levels of other factors were almost unaffected (Figure 3a). These data indicated that circ_0066523 restrained PTEN to activate the PI3K/AKT pathway. To study the impact of the PI3K/AKT pathway on circ_0066523-mediated effects on BMSCs, rescue assays were conducted using insulin-like growth factor 1 (IGF-I), the agonist of this pathway. We found that the dampened proliferation and differentiation of BMSCs due to the loss of circ_0066523 were revived by the overexpression of

IGF-I (Figures 3b to 3d). Together, these data elucidated that circ_0066523 suppresses PTEN to activate PI3K/AKT signalling pathway to propel the proliferation and differentiation of BMSCs.

Circ_0066523 recruits KDM5B to epigenetically repress PTEN transcription. To detect how circ_0066523 induces the repression on PTEN expression, we firstly performed subcellular fractionation assay to determine its distribution in BMSCs. Results indicated that circ_0066523 was located in the cytoplasm and nucleus of BMSCs, but was more abundant in the nucleus (Figure 4a). CircRNAs have been reported to affect gene expression by interacting directly with transcription factors.[21,22] On this basis, we hypothesized that circ_0066523 might epigenetically repress PTEN through transcription factors. Through the UCSC database (University of California, Santa Cruz, USA),[23] we found KDM5B as a potential transcription factor of PTEN (Supplementary Figure ba). Further, we verified the binding affinity between KDM5B and PTEN promoter via chromatin immunoprecipitation (ChIP) assays, demonstrated the overexpression efficiency of pcDNA3.1/KDM5B through qRT-PCR, and proved that upregulating KDM5B reduced the luciferase activity of PTEN promoter (Figure 4b). Moreover, after knockdown efficiency of sh-KDM5B being certified, silencing KDM5B enhanced the protein level of PTEN in BMSCs (Figure 4c). These findings certified the suppression of KDM5B on PTEN transcription in BMSCs. Afterwards, we explored whether circ_0066523 affected PTEN via KDM5B in BMSCs. Interestingly, the RPISeq website[24] suggested that the probability of interaction between KDM5B and circ_0066523 was greater than 0.5 (Supplementary Figure bb). Furthermore, the data from RNA pull down and RIP assays verified the interaction between KDM5B and circ_0066523 in BMSCs (Figure 4d). Of note, circ_0066523 silencing noticeably diminished the binding of KDM5B to PTEN promoter, resulting in increased H3K4me3 occupancy on PTEN promoter (Figure 4e). Importantly, after the overexpression efficiency of pcDNA3.1/circ_0066523 was certified, loss of circ_0066523 remarkably enhanced the luciferase activity of PTEN promoter, while upregulation of circ_0066523 led to the opposite effect (Figure 4f and Supplementary Figure bc). Jointly, we concluded that circ_0066523 recruits KDM5B to transcriptionally repress PTEN expression in BMSCs.

PTEN knockdown counteracts the effects of silenced circ_0066523 on the proliferation and osteoblastic phenotype of BMSCs. We next studied whether circ_0066523 exerted effects on BMSCs via repressing PTEN. Hence, we performed subsequent rescue assays. It was demonstrated that the transfection of sh-PTEN could effectively inhibit the expression of PTEN in BMSCs (Supplementary Figure bd). Importantly, the proliferation of BMSCs inhibited by circ_0066523 deficiency was restored by PTEN knockdown (Figure 5a). We found that Alizarin Red S-stained mineralized nodules, ALP activity, and ALP staining were decreased by circ_0066523 interference, while being increased in response to PTEN knockdown (Figure 5b). Similarly, the expression declination of RUNX2, OCN, and OPN induced by depleted circ_0066523 was also reversed by PTEN downregulation (Figure 5c). Overall, these results showed that PTEN mediates the contribution of circ_0066523 to BMSC proliferation and osteogenic differentiation.

Discussion

In recent years, a growing number of circRNAs have been identified as potential modulators of disease development.[25-28] In our study, circ_0066523 was found to be overexpressed in the osteoblast differentiation induction process of BMSCs. Of note, circ_0066523 knockdown hindered the proliferation and osteogenic differentiation of BMSCs. From the perspective of mechanism, we found that PI3K/AKT signalling pathway was responsible for the biological role of circ_0066523 in BMSCs.

PTEN is a well-established homeostatic regulator that can negatively regulate PI3K/AKT/mechanistic target of rapamycin (mTOR) signalling pathway via its lipid phosphatase activity against phosphatidylinositol (3,4,5)-trisphosphate. Besides, PTEN is essential for cell growth in physiological or pathological situations.[29] It has been reported that PTEN could be epigenetically silenced by some transcription repressor proteins, leading to the activation of PI3K/AKT pathway and the development of diseases. For instance, enhancer of zeste 2 polycomb repressive complex 2 subunit (EZH2) was found to curb PTEN transcription via promoting H3K27me3.[30] From our experimental findings, both the mRNA and protein levels of PTEN were upregulated after silencing of circ_0066523. Further, we identified KDM5B as a transcriptional inhibitor for PTEN. Previously, the negative regulation of KDM5B on PTEN was well-documented in hepatocellular carcinoma cells.[31]

KDM5B, which belongs to the KDM5 / Jumonji/ARID domain-containing protein 1 (JARID1) family, is a specific demethylase for histone H3K4.[32] It affects the expression of target genes via altering the H3K4me3 status in the promoter region. Previously, KDM5B has been found to be an important H3K4-methylome regulator in stem cells as well.[33] In current work, we demonstrated that circ_0066523 recruited KDM5B to inactivate PTEN transcription via decreasing the occupancy of H3K4me3 on PTEN promoter, further leading to the stimulation of the PI3K/AKT pathway. This circ_0066523/KDM5B/PTEN/PI3K/AKT axis emerged as a molecular mechanism responsible for the impacts of circ_0066523 on BMSCs. Consistent with our mechanistic deduction, knockdown of PTEN effectively counteracted the effects of circ_0066523 silencing on BMSC proliferation and osteogenic differentiation.

In short, our study put forward the circ_0066523/KDM5B/PTEN/PI3K/AKT axis for the very first time in the research on the behaviours of BMSCs. This finding may provide the solid theoretical foundation for identifying novel targets of BMSC-related diseases, such as ONFH.

However, lack of in-depth explorations to provide in vivo data or even clinical evidences are the main limitations of the present work.

Supplementary material

Figures showing the induction of bone mesenchymal stem cell osteogenic differentiation and the interaction between circ-0066523 and lysine demethylase 5B.

References

1. **Lee JS**, **Lee JS**, **Roh HL**, **Kim CH**, **Jung JS**, **Suh KT**. Alterations in the differentiation ability of mesenchymal stem cells in patients with nontraumatic osteonecrosis of the femoral head: comparative analysis according to the risk factor. *J Orthop Res*. 2006;24(4):604–609.
2. **Osagie-Clouard L**, **Sanghani-Kerai A**, **Coathup M**, **Meeson R**, **Briggs T**, **Blunn G**. The influence of parathyroid hormone 1-34 on the osteogenic characteristics of adipose- and bone-marrow-derived mesenchymal stem cells from juvenile and ovarectomized rats. *Bone Joint Res*. 2019;8(8):397–404.
3. **Wu T**, **Zhang J**, **Wang B**, **Sun Y**, **Liu Y**, **Li G**. Staphylococcal enterotoxin C2 promotes osteogenesis of mesenchymal stem cells and accelerates fracture healing. *Bone Joint Res*. 2018;7(2):179–186.
4. **Zhang J**, **Hao X**, **Yin M**, **Xu T**, **Guo F**. Long non-coding RNA in osteogenesis: a new world to be explored. *Bone Joint Res*. 2019;8(2):73–80.
5. **Xie X**, **Liu M**, **Meng Q**. Angelica polysaccharide promotes proliferation and osteoblast differentiation of mesenchymal stem cells by regulation of long non-coding RNA H19: an animal study. *Bone Joint Res*. 2019;8(7):323–332.
6. **Qu S**, **Zhong Y**, **Shang R**, **et al**. The emerging landscape of circular RNA in life processes. *RNA Biol*. 2017;14(8):992–999.
7. **Qu S**, **Yang X**, **Li X**, **et al**. Circular RNA: A new star of noncoding RNAs. *Cancer Lett*. 2015;365(2):141–148.
8. **Sun H**, **Xi P**, **Sun Z**, **et al**. Circ-SFMBT2 promotes the proliferation of gastric cancer cells through sponging miR-182-5p to enhance CREB1 expression. *Cancer Manag Res*. 2018;10:5725–5734.
9. **Li Y**, **Wan B**, **Liu L**, **Zhou L**, **Zeng Q**. Circular RNA circMTO1 suppresses bladder cancer metastasis by sponging miR-221 and inhibiting epithelial-to-mesenchymal transition. *Biochem Biophys Res Commun*. 2019;508(4):991–996.
10. **Mao YY**, **Wang JQ**, **Guo XX**, **Bi Y**, **Wang CX**. Circ-SATB2 upregulates STIM1 expression and regulates vascular smooth muscle cell proliferation and differentiation through miR-939. *Biochem Biophys Res Commun*. 2018;505(1):119–125.
11. **Yin Q**, **Wang J**, **Fu Q**, **Gu S**, **Rui Y**. CircRUNX2 through has-miR-203 regulates RUNX2 to prevent osteoporosis. *J Cell Mol Med*. 2018;22(12):6112–6121.
12. **Cherubini A**, **Barilani M**, **Rossi RL**, **et al**. FOXP1 circular RNA sustains mesenchymal stem cell identity via microRNA inhibition. *Nucleic Acids Res*. 2019;47(10):5325–5340.
13. **Shen W**, **Sun B**, **Zhou C**, **Ming W**, **Zhang S**, **Wu X**. CircFOXP1/FOXP1 promotes osteogenic differentiation in adipose-derived mesenchymal stem cells and bone regeneration in osteoporosis via miR-33a-5p. *J Cell Mol Med*. 2020;24(21):12513–12524.
14. **Matsui T**, **Rosenzweig A**. Convergent signal transduction pathways controlling cardiomyocyte survival and function: the role of PI 3-kinase and Akt. *J Mol Cell Cardiol*. 2005;38(1):63–71.
15. **Mukherjee A**, **Rotwein P**. Akt promotes BMP2-mediated osteoblast differentiation and bone development. *J Cell Sci*. 2009;122(Pt 5):716–726.
16. **Srivastava S**, **Sharma K**, **Kumar N**, **Roy P**. Bradykinin regulates osteoblast differentiation by Akt/ERK/NFkappaB signaling axis. *J Cell Physiol*. 2014;229(12):2088–2105.
17. **Tong Y**, **Feng W**, **Wu Y**, **Lv H**, **Jia Y**, **Jiang D**. Mechano-growth factor accelerates the proliferation and osteogenic differentiation of rabbit mesenchymal stem cells through the PI3K/AKT pathway. *BMC Biochem*. 2015;16:1.
18. **Ulici V**, **Hoenselaar KD**, **Gillespie JR**, **Beier F**. The PI3K pathway regulates endochondral bone growth through control of hypertrophic chondrocyte differentiation. *BMC Dev Biol*. 2008;8:40.
19. **Xie S**, **Jiang X**, **Wang R**, **et al**. Low-intensity pulsed ultrasound promotes the proliferation of human bone mesenchymal stem cells by activating PI3K/AKt signaling pathways. *J Cell Biochem*. 2019;120(9):15823–15833.
20. **Ye C**, **Zhang W**, **Hang K**, **et al**. Extracellular IL-37 promotes osteogenic differentiation of human bone marrow mesenchymal stem cells via activation of the PI3K/AKT signaling pathway. *Cell Death Dis*. 2019;10(10):753.
21. **Zang J**, **Lu D**, **Xu A**. The interaction of circRNAs and RNA binding proteins: an important part of circRNA maintenance and function. *J Neurosci Res*. 2020;98(1):87–97.
22. **Yang F**, **Fang E**, **Mei H**, **et al**. *Cis*-Acting *circ-CTNNB1* Promotes β-Catenin Signaling and Cancer Progression via DDX3-Mediated Transactivation of YY1. *Cancer Res*. 2019;79(3):557–571.
23. **No authors listed**. The UCSC Genome Browser. University of California, Santa Cruz Genomics Institute. 2021. http://genome.ucsc.edu (date last accessed 25 June 2021).
24. **No authors listed**. RNA-Protein Interaction Prediction (RPISeq). Iowa State University. 2011. http://pridb.gdcb.iastate.edu/RPISeq (date last accessed 25 June 2021).
25. **Li J**, **Yang J**, **Zhou P**, **et al**. Circular RNAs in cancer: novel insights into origins, properties, functions and implications. *Am J Cancer Res*. 2015;5(2):472–480.
26. **Han B**, **Chao J**, **Yao H**. Circular RNA and its mechanisms in disease: from the bench to the clinic. *Pharmacol Ther*. 2018;187:31–44.
27. **Kumar L**, **Shamsuzzama**, **Haque R**, **Baghel T**, **Nazir A**. Circular RNAs: the emerging class of non-coding RNAs and their potential role in human neurodegenerative diseases. *Mol Neurobiol*. 2017;54(9):7224–7234.
28. **Altesha MA**, **Ni T**, **Khan A**, **Liu K**, **Zheng X**. Circular RNA in cardiovascular disease. *J Cell Physiol*. 2019;234(5):5588–5600.
29. **Pulido R**. PTEN Inhibition in Human Disease Therapy. *Molecules*. 2018;23(2):285.
30. **Li H**, **Ma X**, **Yang D**, **Suo Z**, **Dai R**, **Liu C**. PCAT-1 contributes to cisplatin resistance in gastric cancer through epigenetically silencing PTEN via recruiting EZH2. *J Cell Biochem*. 2020;121(2):1353-1361.
31. **Tang B**, **Qi G**, **Tang F**, **et al**. JARID1B promotes metastasis and epithelial-mesenchymal transition via PTEN/AKT signaling in hepatocellular carcinoma cells. *Oncotarget*. 2015;6(14):12723–12739.
32. **Klein BJ**, **Piao L**, **Xi Y**, **et al**. The histone-H3K4-specific demethylase KDM5B binds to its substrate and product through distinct PHD fingers. *Cell Rep*. 2014;6(2):325–335.
33. **Xhabija B**, **Kidder BL**. KDM5B is a master regulator of the H3K4-methylome in stem cells, development and cancer. *Semin Cancer Biol*. 2019;57:79–85.

Author information:
- W. Xin, PhD, Orthopaedic Surgeon
- S. Yuan, MD, Orthopaedic Surgeon
- B. Wang, PhD, Orthopaedic Surgeon
- Q. Qian, MD, Head of Department
- Y. Chen, MD, Orthopaedic Surgeon

Department of Orthopedics, Changzheng Hospital, Shanghai, China.

Author contributions:
- W. Xin: Writing – original draft.
- S. Yuan: Writing – original draft.
- B. Wang: Investigation.
- Q. Qian: Investigation, Formal analysis.
- Y. Chen: Visualization.

Funding statement:
- This research received no specific grant from any funding agency in the public, commercial, or not-for-profit sectors. No benefits in any form have been received or will be received from a commercial party related directly or indirectly to the subject of this article.

Data sharing:
- Data obtained from this study have been provided in the manuscript and supplementary material.

Acknowledgements:
- We acknowledge the help of all laboratory members in this study.

Open access funding:
- The authors report that the open access funding for their manuscript was self-funded.